PHASE DAMPING IN THE SNS LINAC*

Y. Zhang and S. D. Henderson
Spallation Neutron Source, ORNL, Oak Ridge, TN 37831, U.S.A.

Abstract

Synchronous phase oscillations and the beam phase adiabatic damping curves in the SNS linac are studied with linac models and measured with all the linac beam phase monitors. This study provides a new beam diagnostic technique for detecting RF cavity phase and/or field amplitude errors in a linac with many independently phased cavities. The phase damping curves predicted in the linac longitudinal model could also be utilized to analyze the longitudinal lattice of the superconducting linac - in which each cavity gradient varies widely from the nominal design and a smooth longitudinal focusing is very important to preserve beam emittance in the linac.

INTRODUCTION

The Spallation Neutron Source (SNS) 1-GeV linac consists of a normal conducting front end up to 186-MeV in which a RFQ, 4 rebuncher cavities, 6 drift-tube-linac (DTL) cavities and 4 coupled-cavity-linac (CCL) tanks – a total of 15 normal conducting RF cavities/tanks, and a superconducting linac (SCL) are constructed. Most of the beam energy comes from the SCL with 81 independently phased 6-cell niobium cavities in 23 cryomodules [1]. In the design, the static RF setpoint error is limited within ±1° phase and ±1% field amplitude, while the correlated dynamic RF error needs to be further controlled to within ±0.5° and ±0.5% for each of the linac cavities.

Because of the SRF technique adopted in the SCL, and to achieve a beam energy as high as possible at the SNS, the SC cavity gradients are usually scattered widely – from 0 to 18-MV/m in neutron productions, and smoothing of the longitudinal focus by adjusting the cavity phase is necessary to preserve beam emittance in the linac. This arrangement is different from a normal conducting linac, in which each cavity must always operate at the design gradient and at the design phase. In the SCL, the task of the longitudinal lattice smoothing is usually performed with a fixed phase or a fixed focusing method. But there are generally several SCL cavities that are not operational, and when all the cavities in a whole cryomodule are not available, as in the current situation, longitudinal lattice smoothing becomes very important.

During the linac cavity tune-up process, beam jitters and RF drift always exist. So even if the cavity tune-up algorithm itself could have an accuracy higher than ±1° and ±1% for each individual RF cavity, the actual RF setpoint errors could be larger than that in a proton or heavy ion linac with many independently phased cavities. Human error is also likely, e.g., in one instance, an SCL cavity was set 180° from the design and instead of a beam energy gain of approximately 15-MeV, there was an actual loss of 15-MeV. In another case, a medium-beta-beam-transport (MEBT) rebuncher cavity had a similar error - instead of being bunched, beam was debunched. Detecting these kinds of RF errors in the linac system was a tedious and time consuming task.

We developed a technique for linac longitudinal lattice analysis based on small perturbations. A computer model was built to simulate synchrotron oscillation in the SCL. By introducing appropriate disturbances in the model and applying them to the real machine, we could compare the differences in the beam phase oscillation and damping between the model and the measurement, obtain a picture of the overall quality of the linac longitudinal lattice, and detect systematic errors of the RF setpoints in the linac. All the model development and the beam measurements were completed in 2006 during the SCL commissioning [2]. However, all the details of the work have not been published yet.

In this paper, we will briefly introduce the synchrotron oscillation and adiabatic phase damping in a RF linac and the numerical SCL longitudinal model, discuss the results of lattice analysis with the model against multi-particle tracking simulations, and compare the model predictions with the results of all the linac beam phase monitor (BPM) measurements.

PHASE DAMPING AND LINAC MODEL

The theory of longitudinal motion of charged particles in an RF acceleration structure is extensively discussed in most accelerator physics text books. Here, we briefly summarize beam synchrotron oscillation and adiabatic phase damping in a constant acceleration RF structure. For small acceleration approximations ($\delta\beta << 1$), the second-order differential equation for the particle phase motion in an RF acceleration structure is described by [3]:

$$\frac{d^2\phi}{dz^2} = -\frac{2\pi \cdot qE_0T}{mc^2\beta^3\gamma^3\lambda} \cdot (\cos\phi - \cos\phi_S) \qquad (1)$$

where, z is the axial distance and q is the particle charge, E_0 is the integrated gradient over the RF structure, T is the transient time factor (TTF), ϕ_S is the synchronous phase, mc^2 is the rest energy, β and γ are relativistic factors of the beam, and λ is the free space RF wavelength.

The stable solution of Equation (1) defines an RF bucket and the maximum energy half-width of its separatrix occurs for $\phi = \phi_S$:

$$\frac{\Delta W_{MAX}}{mc^2} = \sqrt{\frac{2qE_0T\beta^3\gamma^3\lambda}{\pi \cdot mc^2}(\phi_S\cos\phi_S - \sin\phi_S)} \qquad (2)$$

* SNS is managed by UT-Battelle, LLC, under contract DE-AC05-00OR22725 for the U.S. Department of Energy.

Phase damping is the effect of phase amplitude decrease and energy amplitude increase of synchrotron oscillations during particle acceleration in an RF linac. In the small-amplitude synchrotron oscillations ($|\phi - \phi_S| << 1$) for a constant acceleration gradient and a fixed cavity synchronous phase, it is simplified as:

$$\phi_0 - \phi_S = \frac{cons\tan t}{(\beta\gamma)^{3/4}} \quad (3)$$

where, ϕ_0 is the maximum phase.

The acceleration gradient of a SCL cavity is in the range of 10 to 20-MV/m, which is not so small. The small acceleration approximation serves only as a reference at here. An SCL longitudinal model is developed to simulate particle acceleration and beam phase variations in the linac. The model utilizes thin lens approximation [4] to compute particle acceleration in a cavity: the particle is assumed to travel at constant velocity to the cavity center, where it receives a longitudinal kick and is then transported out of the cavity at a new velocity. The energy gain and phase change in a cavity is computed from the following equations:

$$\Delta W = qE_0 \cdot T \cdot L \cdot \cos\phi_S$$
$$\Delta\phi = \frac{qE_0 \cdot L}{mc^2 \cdot \beta^2 \cdot \gamma^3} k \cdot T' \cdot \sin\phi_S \quad (4)$$

where, L is the length of the cavity, k is the wave number, β and γ are the relativistic factors at the center, T and T' are the TTFs that may be computed from acceleration field profile measurements or from cavity design codes such as SUPERFISH [5], and $\Delta\phi$ is the phase kick due to beam acceleration in the cavity.

The model is developed in C++. It uses an extra iteration to determine the absolute phase at each cavity entrance according to the injection energy, E_0 and ϕ_S, and computes the proper RF driven phase for every cavity based on time of flight for the reference particle. The main iteration cycle calculates particle transport and acceleration in the linac using the RF driven phase generated in the previous iteration, but with the actual beam arrival phase. When any parameter changes (beam energy, cavity amplitude or phase), beam phase in all the downstream cavities is affected, similar to the real linac. A matched linac lattice generally shows a damping curve following Equation (3) or at least roughly, but a mismatch due to either an improper longitudinal lattice design or RF setpoint errors, if it is significant, will generate a different synchrotron oscillation that can be detected by a simple comparison with the longitudinal model.

Figure 1 shows RMS beam phase oscillation and damping in the normal conducting linac in the simulation with IMPACT [6] for linear map and zero beam current. The only exception in the damping curve is at the front of DTL1, where synchronous phase ramps up from -45° to -30° to capture the RFQ beams. It is possible to measure the damping curves with many bunch shape monitors (BSMs) along the entire linac, but using linac BPMs will be more convenient with appropriate beam perturbations introduced into the linac, because oscillation of the beam phase centroid follows the same damping but at half the frequency. Figure 2 shows the phase centroid oscillation and damping in the baseline SCL in the simulation with the longitudinal model, simply from reducing the gradient of the first cavity and doing nothing to all the other cavities. Because the TTF varies during the particle accelerations, and gradients of the medium beta cavity and the high beta cavity are quite different, the damping curve is not a pure adiabatic one, but approximate.

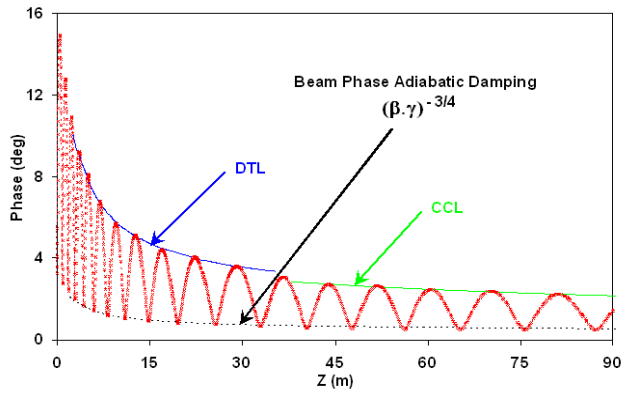

Fig. 1. Phase damping in the normal donducting linac.

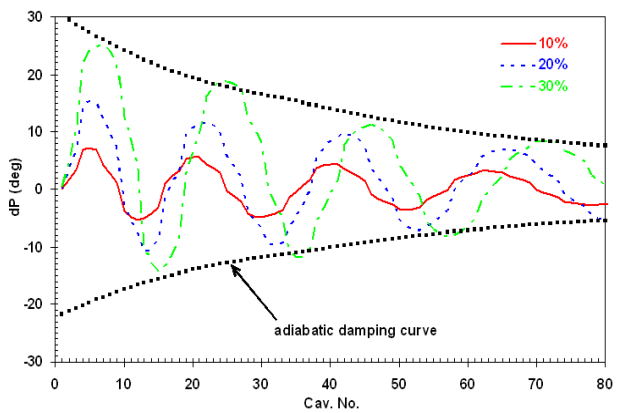

Fig. 2. Phase centroid oscillations and damping in SCL.

PARTICLE TRACKING SIMULATION

The first application of the linac model is the study of dynamic RF errors in the SCL, which are different from the static RF setpoint errors. Static error is usually isolated within each cavity and is generated during the cavity tune-up. While dynamic error (e.g., beam phase) also depends on all the upstream cavities, it changes constantly and is concerned in routine operation. For the baseline SCL design, it is known that static error in cavity amplitude of up to 30% is tolerable [7]. However, dynamic error of only 5% would be a disaster [8]. Figure 3 shows beam phase oscillation in the baseline SCL model (ϕ_S = -20°; medium beta, E_0T = 10 MV/m; high beta, 16 MV/m) versus coherent cavity amplitude errors. Beams are out of the RF bucket when the

amplitude of all the SC cavities drops by approximately 4.6%. Dividing the beam energy gain by the estate length of the medium beta cryomodule and putting it into Equation (2) may give a similar result.

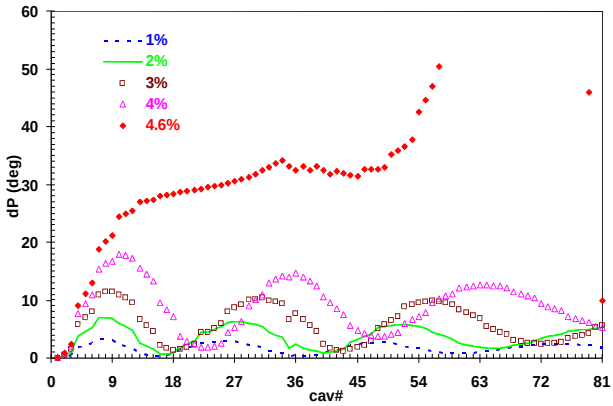

Fig. 3. Phase oscillation in the baseline SCL with cavity amplitude coherently reduced by 1, 2, 3, 4 and 4.6%.

In beam commissioning, most of the SCL cavities are far away from the baseline design gradient (the difference is from -100% to +80%), linac longitudinal focusing is different. Figure 4 shows the synchrotron oscillation and phase damping in the longitudinal model for one of the SCL commissioning lattices. It is mismatched - instead of damping, the amplitude of phase synchrotron oscillation increases at around cavity #20 and #30. The problem is that beam bunching in the first half medium beta section is stronger than in the second half, while the high beta section is weaker than the medium beta counterpart when the fixed phase algorithm is selected. The mismatches and beam space charge effects caused beam emittance dilutions in the longitudinal space in the simulation with the IMPACT code, as shown in Fig. 5. The baseline SCL design lattice is also shown in the figure as a comparison.

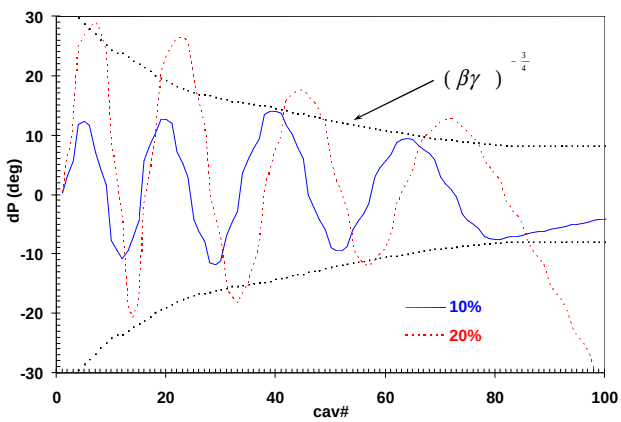

Fig. 4. Abnormal damping in one of the SCL lattices.

Beam transverse emittance is preserved in both cases. However, longitudinal emittance of the commissioning lattice is diluted in the middle of the medium beta section and at the entrance of the high beta section which is coincident to the analysis of mismatches with the phase damping simulations mentioned above. Because the beam current is only 20-mA in the beam commissioning – not very high, these longitudinal mismatches did not cause any transverse emittance dilution, but they could become a problem for neutron production because of space charge effects and the longitudinal-transverse space coupling for high intensity beams. Longitudinal emittance in the SCL commissioning lattice increases rapidly downstream of the linac, it almost doubles that of the baseline design, as the result of the upstream mismatch and the effect of space charge.

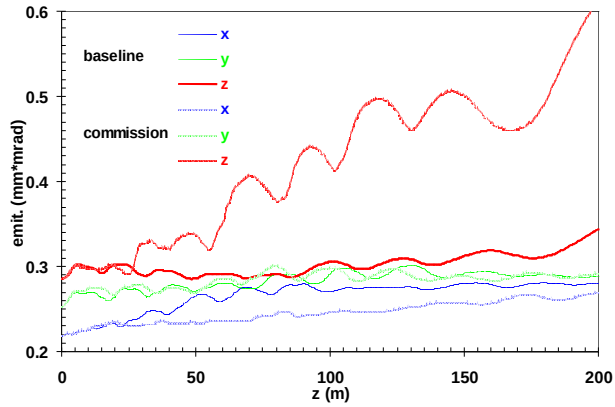

Fig. 5. Beam emittance in the SCL design lattices.

Figure 6 shows the phase damping curves in the SCL for the most recent neutron production. Because the SCL cavity gradient has been changed significantly since the beam commissioning 2 or 3 years earlier, both fixed phase and fixed focusing algorithms may preserve the beam emittance in the linac. They are verified in the simulations with the IMPACT code and in the neutron production operation.

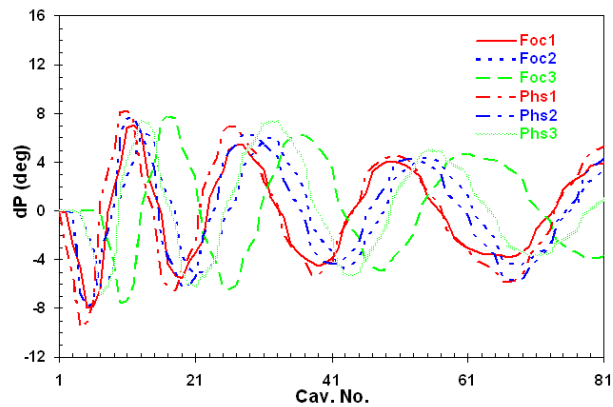

Fig. 6. Phase damping in the SCL production lattice.

LINAC BPMS MEASUREMENTS

The SCL longitudinal model is used to determine static RF setpoint error in the linac by introducing appropriate disturbances to the model, and to the acutal equipment,

and analyzing the differences between the model and the measurement. Figure 7 shows an example of simulations with the baseline SCL. It is obvious that phase or amplitude static setpoint error of a single cavity and random RF errors of all cavities up to a few degrees and a few percent could generate a different synchrotron oscillation in the linac. It reveals that any static RF error changing the synchrotron oscillation in the linac beyond the BPM accuracy could be detected.

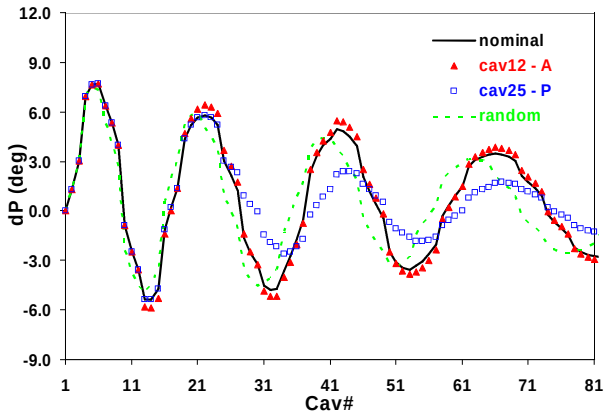

Fig. 7. Phase oscillation in the SCL model. No RF error (nominal); cavity 12 amplitude error of 30% (cav12 –A); cavity 25 phase error 100° (cav25 –P) and random static RF errors of 3° and 5% (random).

The principle of detecting RF setpoint error with the phase oscillation and phase damping study is similar to signature matching. However, instead of matching BPM pairs for a single cavity with an unknown RF setpoint, the phase damping study actually matches all the available BPMs for all the tuned cavities in a linac. When a deviation occurs, it shows that an RF problem happened and where it started. It might be difficult to calculate RF errors directly from the phase damping, because there are too many variables to fit in the linac, but the method is effective for locating the source of the RF error, which is equally important, particularly in a linac with many independently phased cavities. By tracing the phase oscillation upstream to the location where the deviation began, one may determine the RF error with other techniques, such as phase scan and drifting beam.

Figure 8 shows one of the SCL design lattice against the linac BPM measurement for 186-MeV, 15-mA proton beams with a pulse length of approximately 30-μs and the gradient of the first cavity is reduced by 10 and 15% respectively, to generate the centroid oscillations. In the linac BPM measurements, it is noted that the deviation actually occurs at the beginning of the SCL. We have two assumptions: first, the actual change of the first cavity gradient is larger than that of the RF reading; second, beam bunching of the linac at the first 20-m is weaker than in the design. Figure 9 shows the phase oscillation with gradient of the first cavity changed by 12 and 20%, respectively, in the linac longitudinal model. Although it agrees much better with BPMs at the first 20-m, there is no improvement in the downstream lattice. Beam-based calibration shows that gradient of the first cavity is in close agreement with that of the RF calibration (~1%), and we have to discard this assumption.

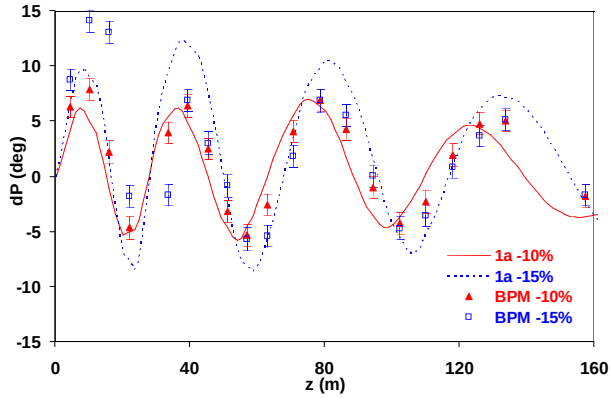

Fig. 8. Phase oscillation in design and in measurement.

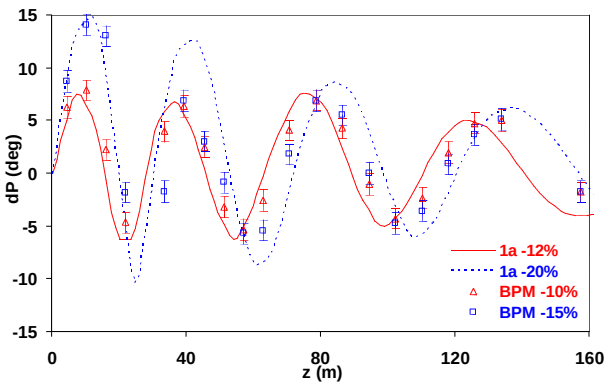

Fig. 9. Cavity gradient change of 12 and 20% in model.

Synchronous phase of all cavities in the first 20-m are increased by 3° in the linac model to study the second assumption, and the result is shown in Fig. 10. In the simulation, approximately 1% gradient error remains in the first cavity, and the model matches the entire linac better than could be expected in the beam commissioning. We verified the RF setpoints of all 12 cavities at the first 20-m SCL, and found out that the synchronous phase of all cavities are shifted by several degrees with an average of approximately 2.2°, which reasonably agrees with the model prediction.

Figures 11 and 12 show model predictions versus the linac BPM measurements for phase oscillations with the cavity 3c and cavity 12a gradient reductions. It is seen that the error bars in the BPM phase measurements are large because of beam jitters and BPM noises, and some measurements may have bad BPM data (e.g., those circled in Fig. 12). We tried several measurements, but did not have a single instance of perfect agreement between the model prediction and the BPM measurement. This is imaginable in beam commissioning because RF

drifts as much as 5° in phase were easily measurable in the SCL. Therefore, the measurements were always dominated by random RF errors, which were also expected from the simulation. We could not isolate the RF drift during the time-consuming linac cavity tune-up procedure, and some errors in the linac longitudinal model could not be excluded completely either. There are other things that could be tried to improve the accuracy, such as averaging a few ten beam pulses to reduce the BPM measurement errors. But unfortunately, a chipmunk was tripped because of excessive beam loss in the linac when we attempted to do so for the first time, raising safety concerns.

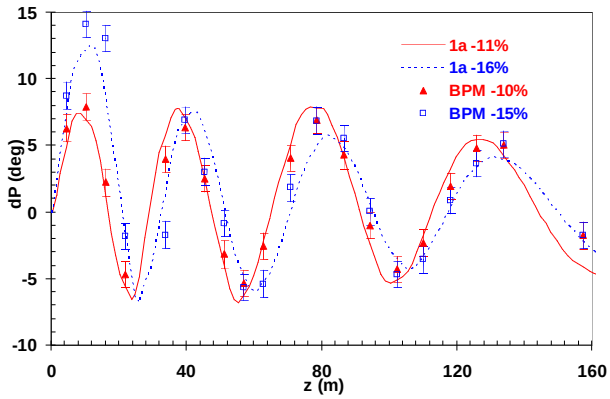

Fig. 10. Model prediction versus BPM measurement.

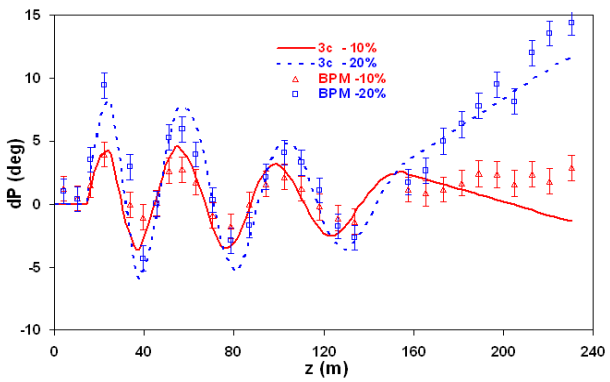

Fig. 11. SCL cavity 3c gradient reduce 10 and 20%.

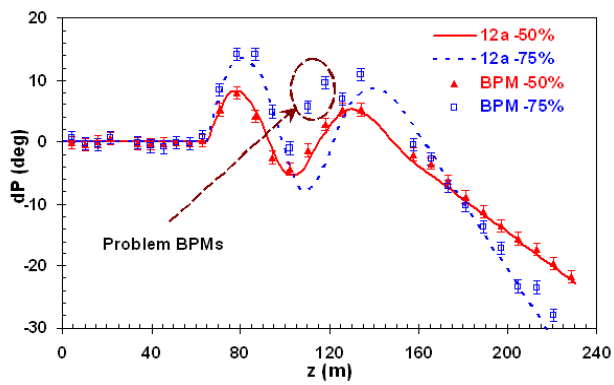

Fig. 12. SCL cavity 12a gradient reduce 50 and 75%.

It was found later that the beam loss was caused by the 180° phase error in one of the MEBT bunchers, and not directly by the phase damping study itself. But it shows one disadvantage of the phase damping study: only the beam centroid matters, and it may not provide information about the beam distribution, which is beyond the scope of this technique. Also note that when the beam energy is highly relativistic, a phase damping study cannot provide much information about the longitudinal lattice nor reveal any RF error, because in that case the beam velocity change is tiny. This method is limited to low and medium energy proton or heavy ion linear accelerators with multiple independently phased RF cavities. Figure 13 shows a phase damping curve measured for a 2.5-MeV, 15-mA injection beams with all the BPMs in the normal conducting linac, where there are few BPMs and this measurement is insufficient to precisely record the synchrotron tunes. To do that accurately, a longitudinal model of the normal conducting linac should be built.

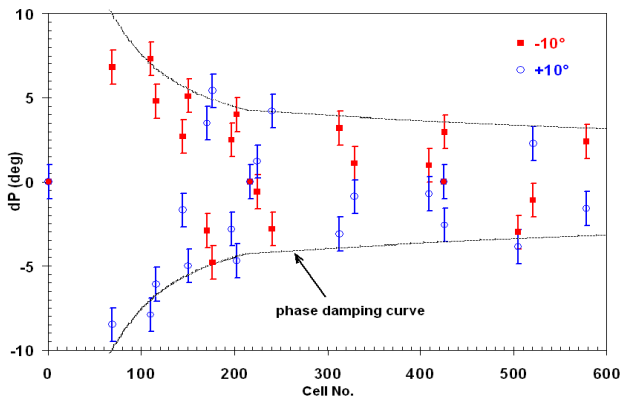

Fig. 13. Phase damping measured in the nc. linac.

The advantage of the phase damping study is it shows a whole picture of the overall longitudinal lattice, though it may not necessarily provide accurate phase and gradient information for each individual RF cavity. The former is also very important to the SCL longitudinal lattice design: each cavity has six cells and, in most cases, none of the cell phases equals the cavity synchronous phase; the phase at the two end cells may differ by more than 100° (Fig. 14). In a correctly tuned cavity, however, the effects of the phase "error" of all the cells cancel each other so that a smooth longitudinal lattice can still be established through the entire linac system. In the SNS linac, there are a total of 96 RF cavities\tanks with more than 1,000 acceleration gaps\cells; therefore more chance to cancel or multiply the RF errors in a local zone. A phase damping study could show the combined effects of all these cavities, which is particularly helpful when many cavities are not functional in the SC linac.

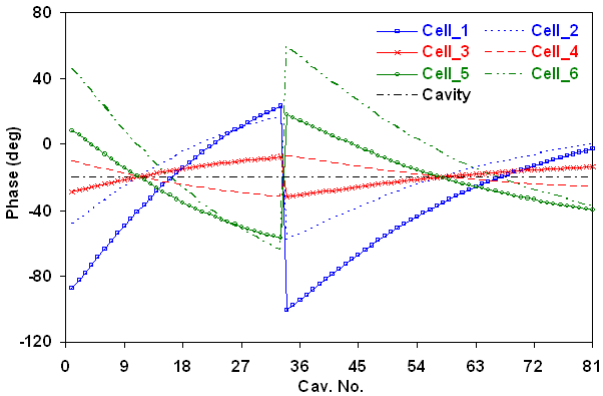

Fig. 14. Phase change in each cell in the baseline SCL.

CONCLUSION

From measurements of beam synchrotron oscillation and phase damping, the longitudinal lattice of the entire linac system and systematic errors of the SCL cavity setpoints are analyzed with the aid of a computer model. The study provides a whole picture for improving the longitudinal lattice for beam acceleration in the linac, and may also be helpful to the cavity tune-up procedure. The principle applies to all other low and medium energy proton or heavy ion linacs in which an RF cavity setpoint error has significant influence on the beam velocity, and in which a smooth longitudinal lattice is critical to preserve beam emittance.

ACKNOWLEDGEMENT

The authors are grateful to A. Aleksandrov, P. Chu, J. Galambos, Z. Kursun, T. Pelaia, A. Shishlo, and many other staff members of the SNS Accelerator Physics and Accelerator Operations groups for support and helpful discussions.

REFERENCES

[1] S. Henderson, proceedings Utilisation and Reliability HPPA (2004) 257.
[2] Y. Zhang, et al, Nuclear Instruments & Methods in Physics Research B, Vol.261 (2007) 1036.
[3] T. P. Wangler, *Principles of RF Linear Accelerators*, John Wiley & Sons, (1998) 175-187.
[4] B. Schnizer, Particle Accelerators, Vol.2 (1971) 141.
[5] J. Billen, L. Young, LA-UR-96-1834, LANL (2000).
[6] J. Qiang, et al, Journal of Computational Physics, Vol. 163 (2000) 434.
[7] S. Nath, et al, proceedings of the European Particle Accelerator Conference, EPAC (2002) 1031.
[8] Y. Zhang, S. Henderson, proceedings of the Linac Conference, Linac (2006) 423.

`